Electronic Supplementary Material (ESI) for Organic & Biomolecular Chemistry.

Supporting information

Thermal Stability of G-rich Anti-parallel DNA Triplexes upon Insertion of LNA and *α*-L-LNA

Tamer R. Kosbar, Mamdouh A. Sofan, Laila Abou-Zeid, and Erik B. Pedersen

Table 1. Results of Mass spectrometry analysis of ONs synthesized.

Sequence	Calculated m/z	Observed m/z
5′GAAGGAGGAGA-TTTT-AGAG**G**^{L}AGGAAG3′	8265.40	8270.58
5′GAAGGAGGAGA-TTTT-AGAGG**A**^{L}GGAAG3′	8265.40	8266.25
5′GAAGGAGGAGA-TTTT-AGAGG**T**^{L}GGAAG3′	8256.40	8259.21
5′GAAGGAGGAGA-TTTT-AGAGG**T**$^{\alpha}$GGAAG3′	8256.40	8257.02
5′GAAGGA**G**^{L}GAGA-TTTT-AGAGGAGGAAG3′	8265.40	8268.89
5′GAAGG**A**^{L}GGAGA-TTTT-AGAGGAGGAAG3′	8265.40	8266.25
5′GAAGG**A**^{L}GGAGA-TTTT-AGAGG**A**^{L}GGAAG3′	8293.28	8297.94
5′GAAGGA**G**^{L}GAGA-TTTT-AGAG**G**^{L}AGGAAG3′	8293.17	8293.98
5′GAAGG**A**^{L}GGAGA-TTTT-AGAGG**T**$^{\alpha}$GGAAG3′	8284.40	8285.40
5′GAAGGAGGAGA-TTTT-AGAGG**T**$^{\alpha}$GGAAG3′	8256.24	8263.64
5′GAAGGAGGAGA-TTTT-AGAGG**T**^{L}GGAAG3′	8256.24	8256.40
5′GAAGG**A**^{L}GGAGA-TTTT-GAGAGGAAAGA3′	8249.40	8251.73
5′GAAGGA**G**^{L}GAGA-TTTT-GAGAGGAAAGA3′	8249.40	8249.77
5′GAAGG**A**^{L}GGAGA3′	3507.26	3502.80
5′GAAGGA**G**^{L}GAGA3′	3507.26	3507.99
5′TCTCC**T**^{L}CCTTC3′	3222.10	3222.83
5′TCTCC**T**$^{\alpha}$CCTTC3′	3222.10	3222.99
5′TC**T**^{L}CC**T**^{L}CC**T**^{L}TC3′	3278.10	3275.69
5′TC**T**$^{\alpha}$CC**T**$^{\alpha}$CC**T**$^{\alpha}$TC3′	3278.10	3274.98
5′TCTC**C**^{L}TCCTTC3′	3236.20	3235.98
5′T**C**^{L}TC**C**^{L}TC**C**^{L}TTC3′	3320.20	3317.69
5′TCTC**C**$^{\alpha}$T**C**CTTC3′	3236.20	3230.29
5′T**C**$^{\alpha}$TC**C**$^{\alpha}$TC**C**$^{\alpha}$TTC3′	3320.20	3314.79
5′T**C**$^{\alpha}$**T**$^{\alpha}$C**C**$^{\alpha}$**T**$^{\alpha}$C**C**$^{\alpha}$**T**$^{\alpha}$TC3′	3404.30	3401.66

MALDI-TOF analysis was performed on a Ultraflex II TOF/TOF system from Bruker (a MALDI-LIFT system) with HPA matrix (10 mg 3-hydroxypicolinic acid, in 50 mm ammonium citrate/70% MeCN).

Thermal Denaturation Studies

Thermal melting measurements were performed on a Perkin-Elmer UV/VIS spectrometer Lambda 35 fitted with a PTP-6 temperature programmer. Melting experiments were performed on equimolar amounts of the appropriate oligonucleotides (target sequence and hairpin) (3 μM) in a buffer solution consisting of sodium cacodylate (10 mM), EDTA (0.1 mM), and $MgCl_2$ (50 mM) at pH 7.2. The solutions were heated to 90 ^oC then cooled down slowly to room temperature, and were then kept at this temperature for 2 h. The absorbance of the formed triplexes was measured at 260 nm with a heating rate of 0.5 ^oC/min. The melting temperature (T_m) was determined as the maximum of the first derivative plots of the melting curves.

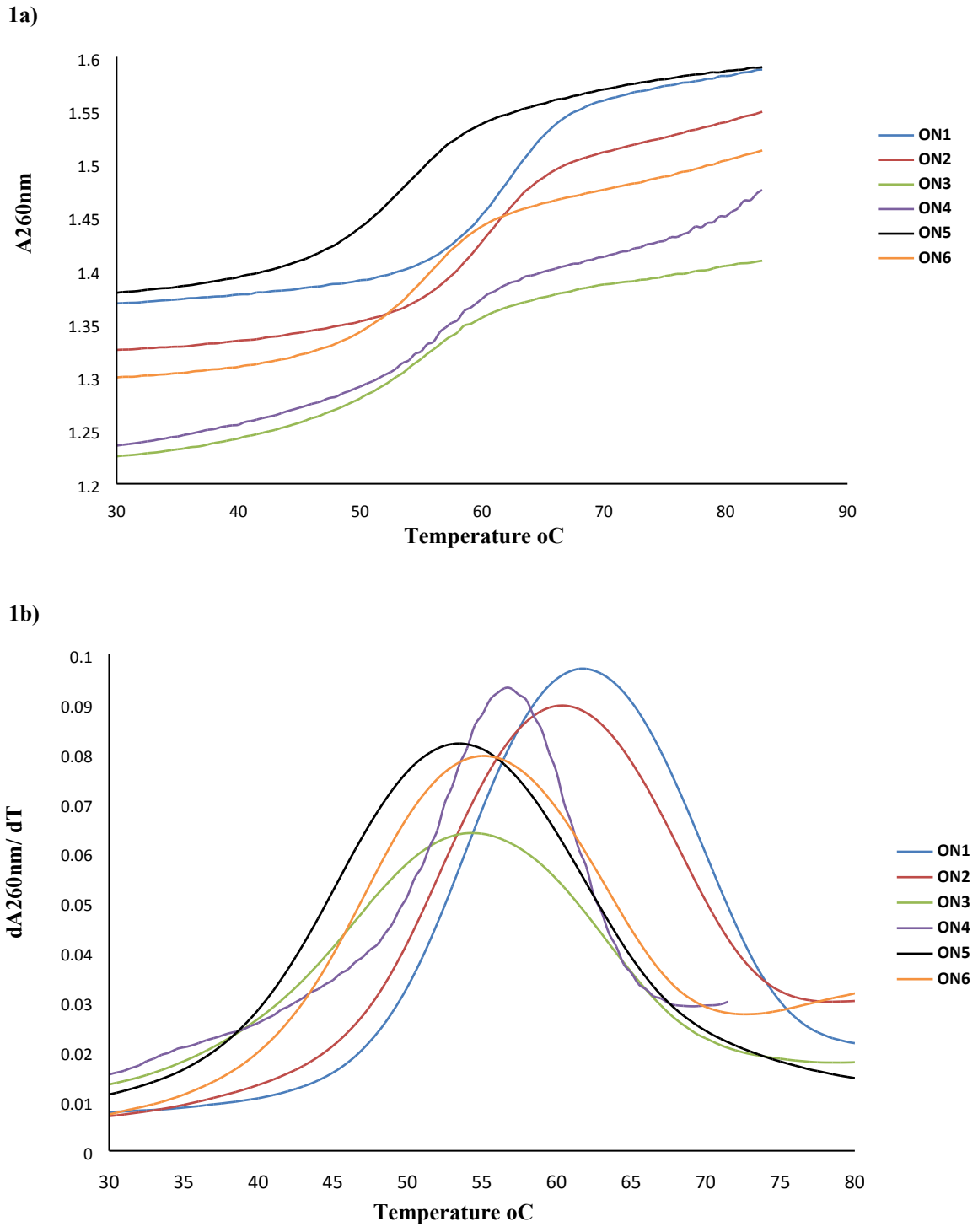

Fig. 1: a) Melting curves of **ON1-ON6**; **b)** Melting curve first derivatives of **ON1-ON6**

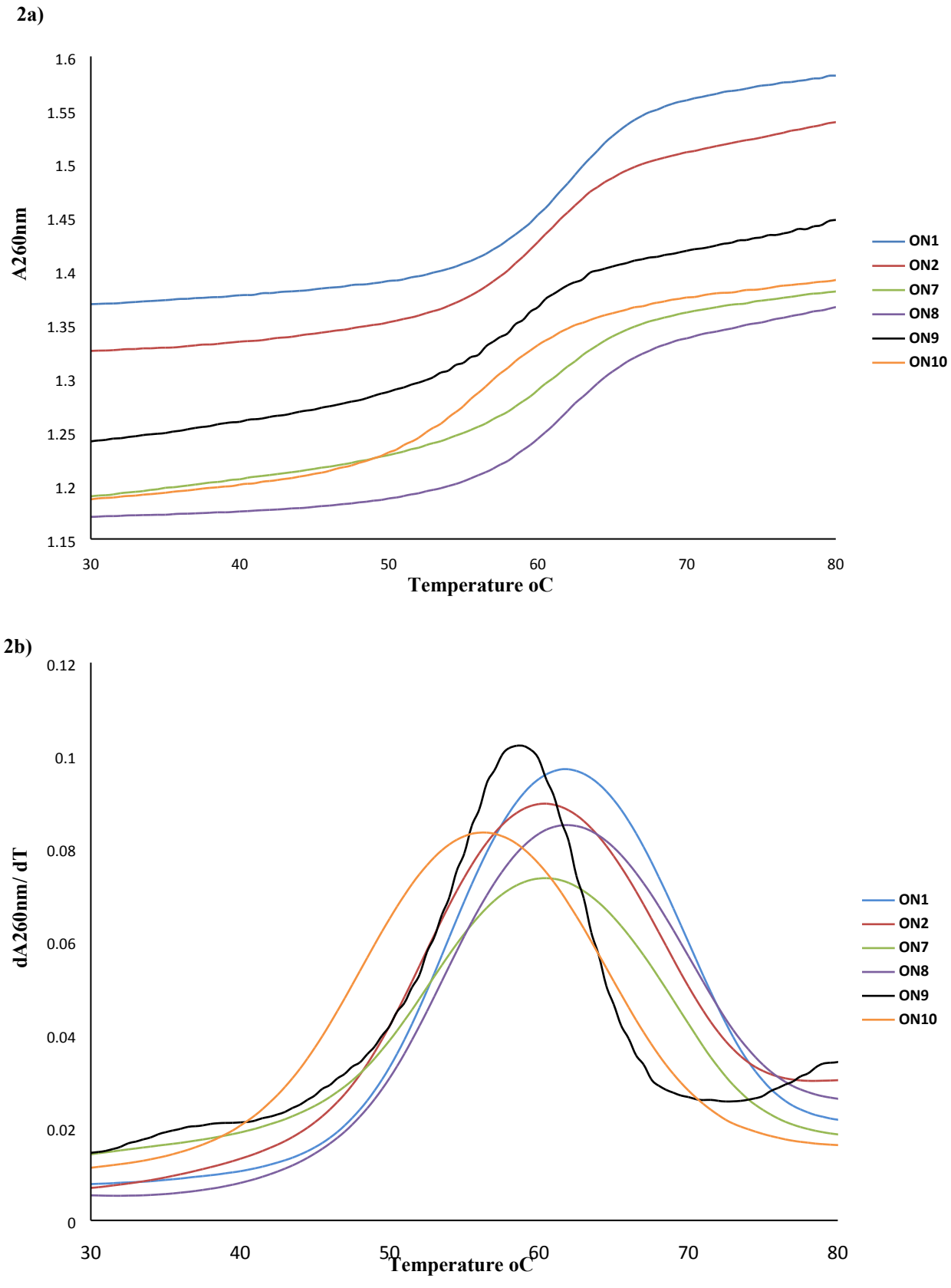

Fig. 2: a) Melting curves of **ON1, ON2** and **ON7-ON10**; **b)** Melting curve first derivatives of **ON1, ON2** and **ON7-ON10**

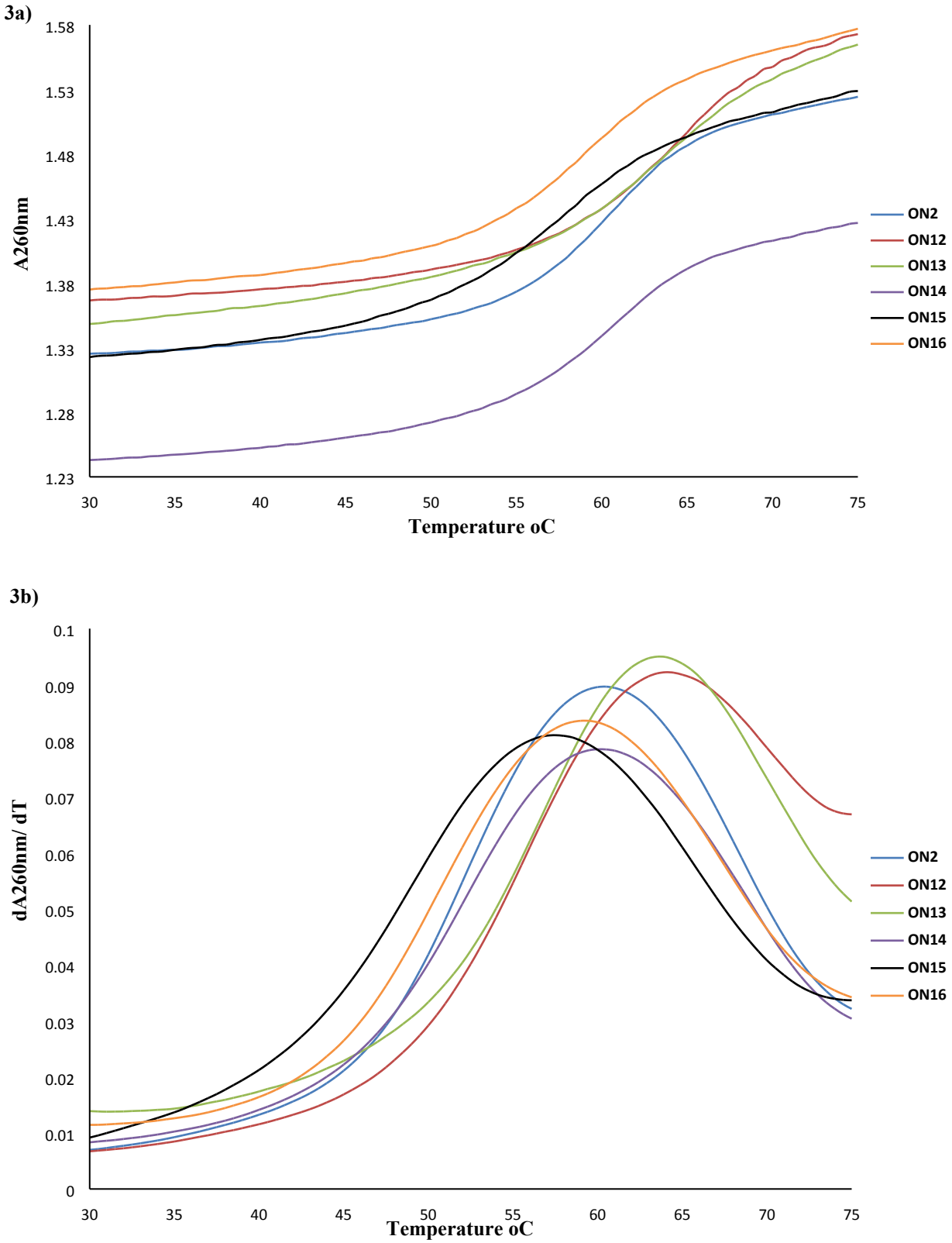

Fig. 3: a) Melting curves of **ON2** and **ON12-ON16**; **b)** Melting curve first derivatives of **ON2** and **ON12-ON16**

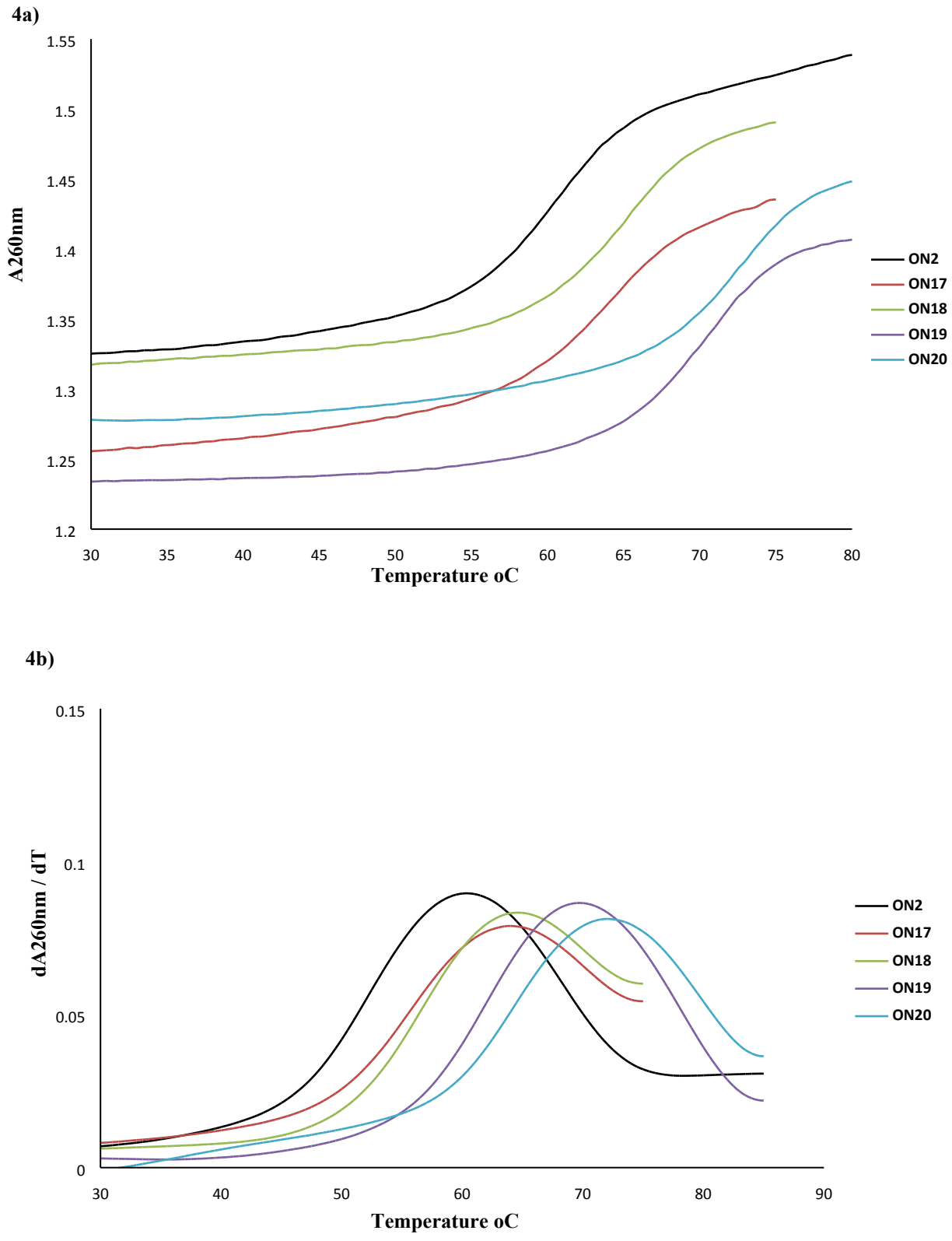

Fig. 4: a) Melting curves of **ON2** and **ON17-ON20**; **b)** Melting curve first derivatives of **ON2** and **ON17-ON20**

5a)

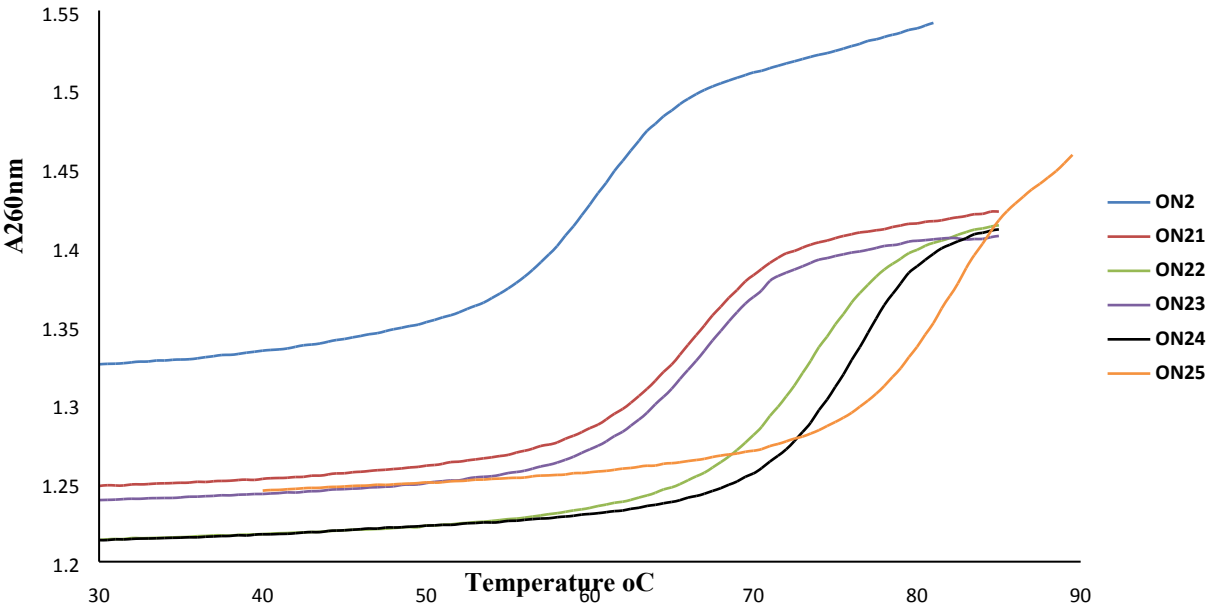

5b)

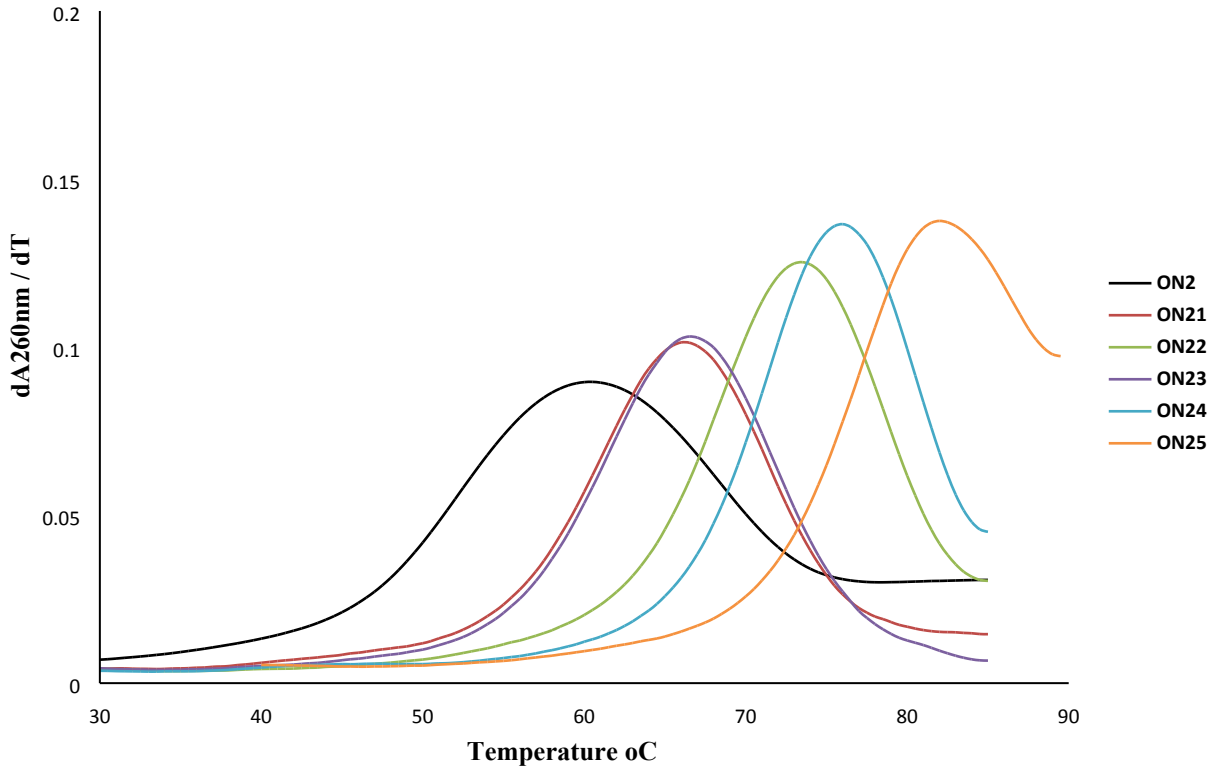

Fig. 5: a) Melting curves of **ON2** and **ON21-ON25**; **b)** Melting curve first derivatives of **ON2** and **ON21-ON25**

6a)

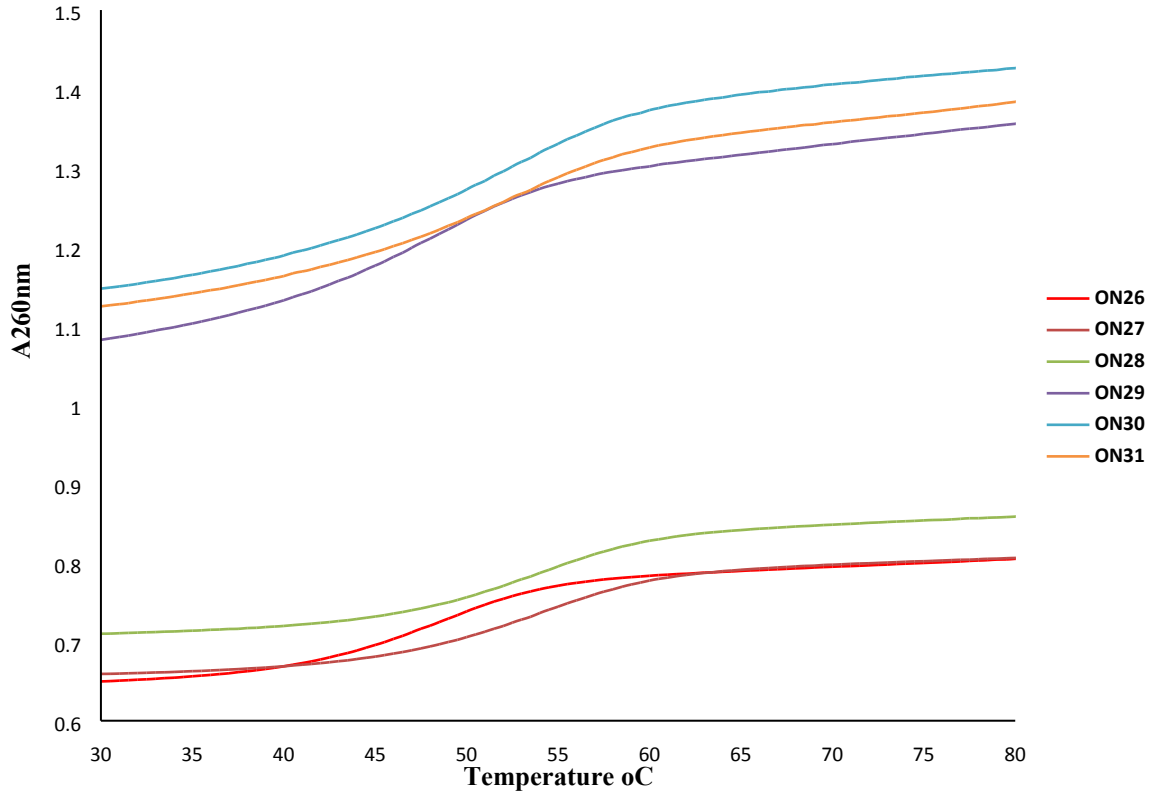

6b)

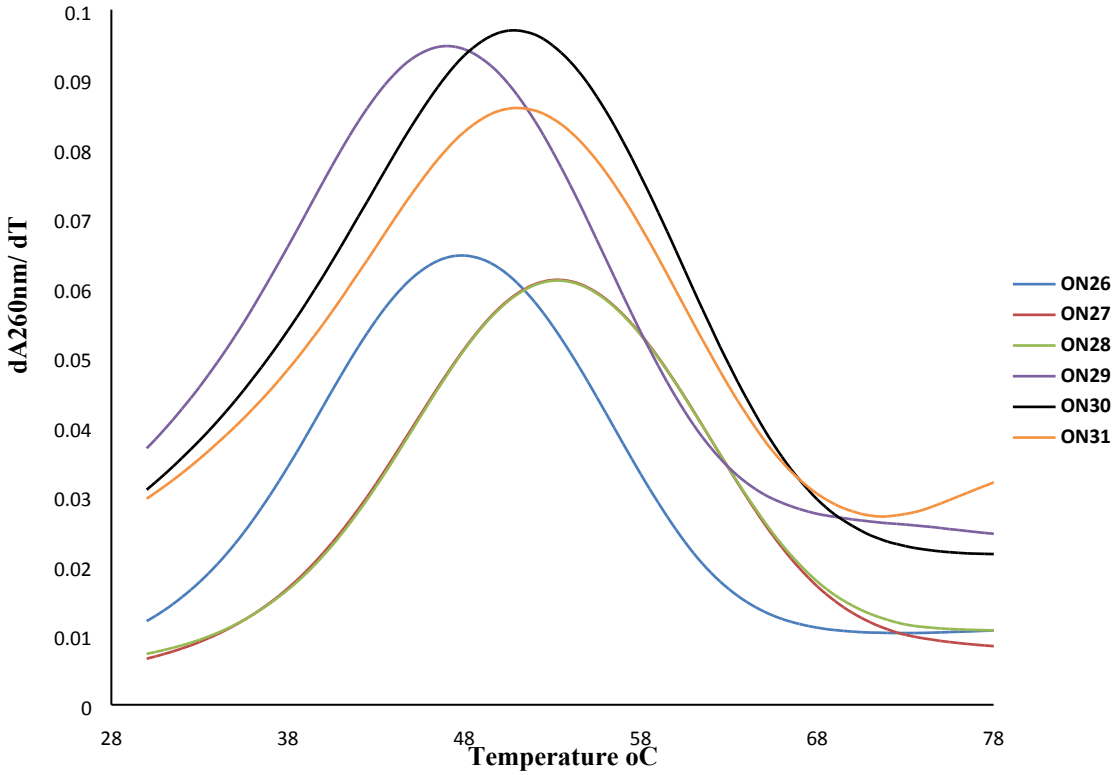

Fig. 6: a) Melting curves of **ON26-ON31**; **b)** Melting curve first derivatives of **ON26-ON31**

7a)

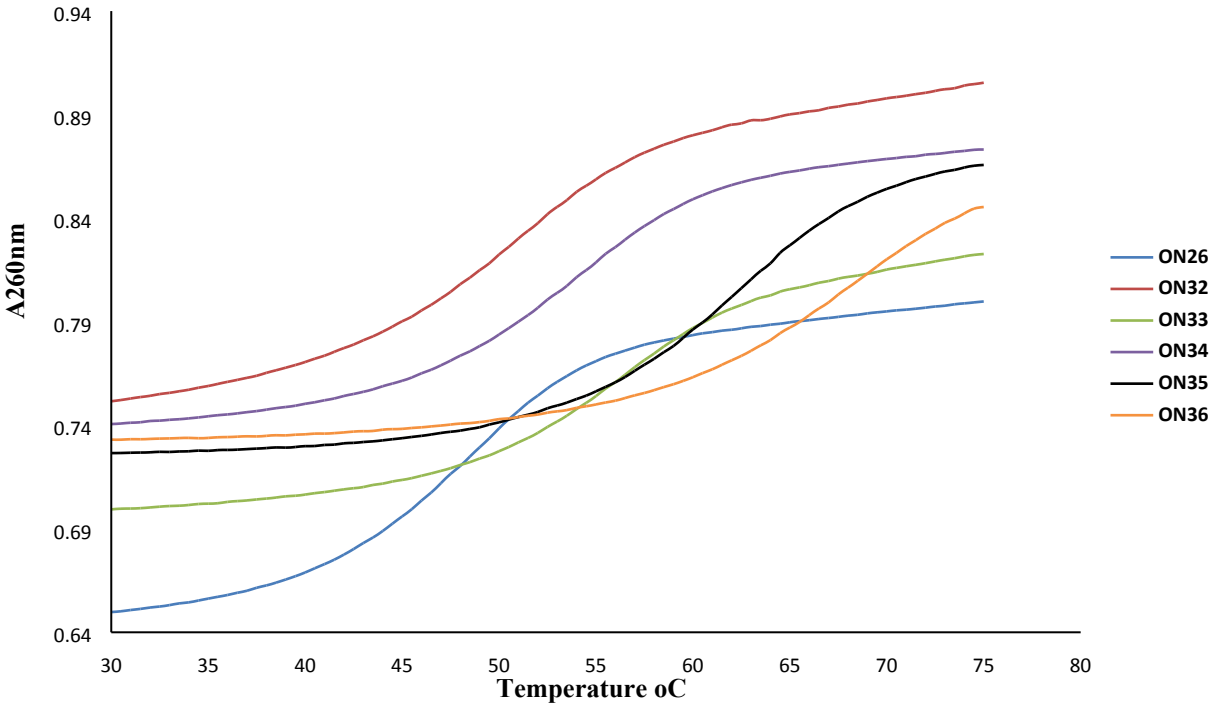

7b)

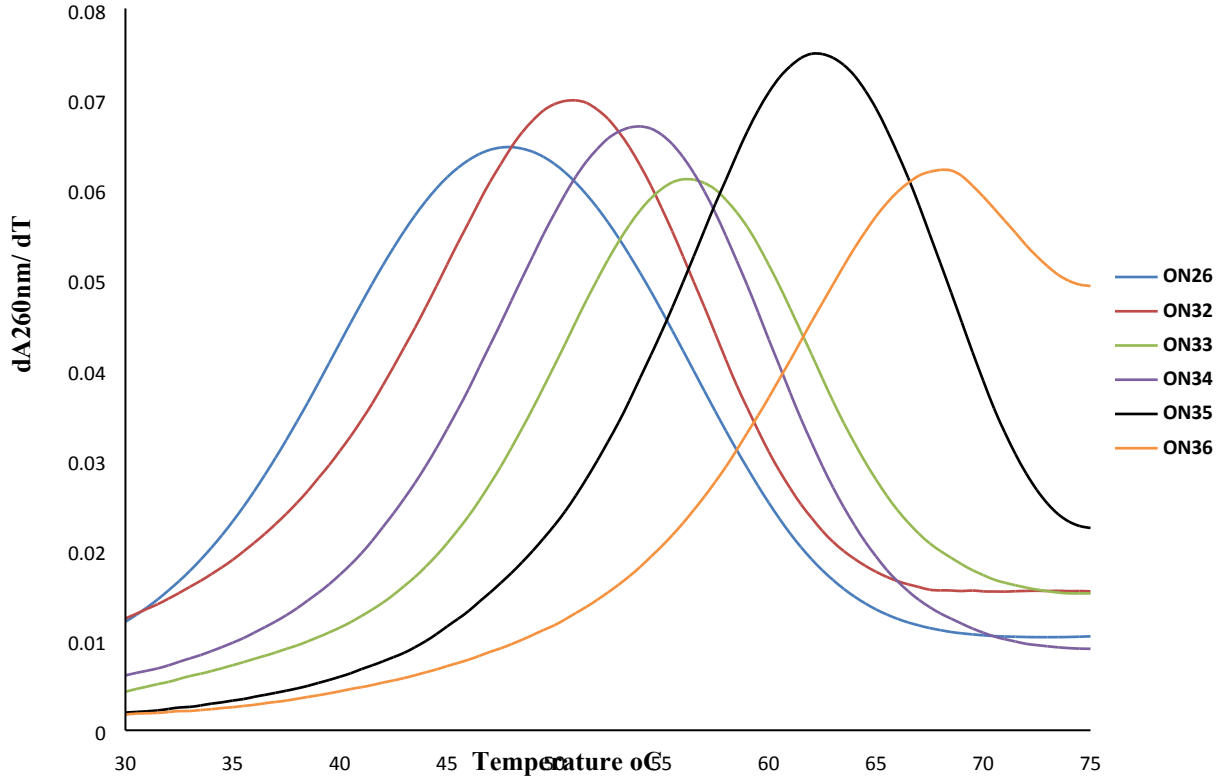

Fig. 7: a) Melting curves of **ON26** and **ON32-ON36**; **b)** Melting curve first derivatives of **ON26** and **ON32-ON36**

Circular Dichroism Spectra (CD)

Circular dichroism spectra were collected on a Jasco J-600A spectropolarimeter using 1 mL quartz cuvettes with 5-mm path length. Oligonucleotides (3 μM) were mixed in a buffer solution consisting of sodium cacodylate (10 mM), EDTA (0.1 mM), and $MgCl_2$ (50 mM) at pH 7.2. All samples were annealed for 2 minutes at 80 °C and slowly cooled to room temperature before data collection. Measurements were performed at 20 °C in the 200–350 nm wavelength range with a continuous scanning mode, 50 nm/min as a scanning speed, 4 sec for a response and accumulation 5 times. The buffer spectrum was subtracted from the sample spectra.

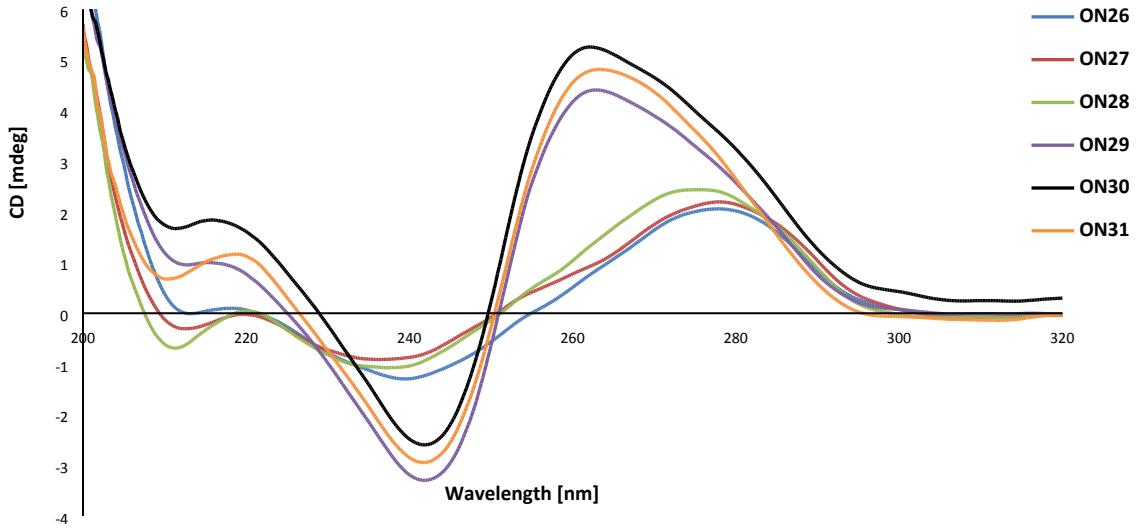

Fig. 8: CD spectra of ON26-ON31

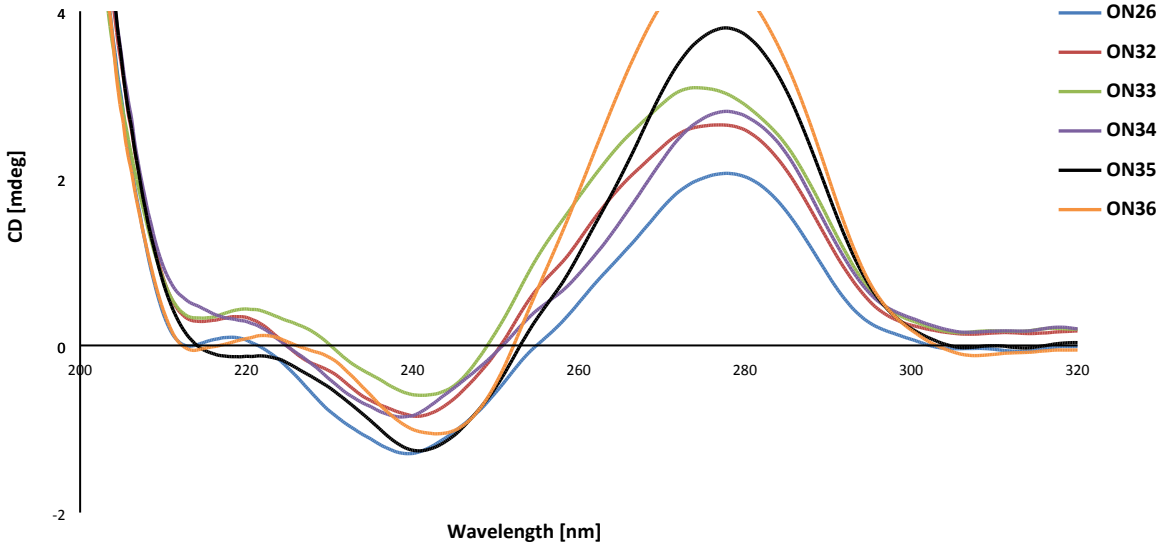

Fig. 9: CD spectra of ON26 and ON32-ON36

Molecular modeling

Molecular modeling was performed with Macro Model v9.1 from Schrödinger. All calculations were conducted with AMBER* force field and the GB/SA water model. The dynamic simulations were performed with stochastic dynamics, a SHAKE algorithm to constrain bonds to hydrogen, time step of 1.5 fs and simulation temperature of 300 K. Simulation for 0.5 ns with an equilibration time of 150 ps generated 250 structures, which all were minimized using the PRCG method with convergence threshold of 0.05 kJ/mol. Patel's structure of the anti-parallel triplex[32] was downloaded from the protein data bank (PDB entry pdb134d), followed by incorporation of the nucleobases $\mathbf{T^L}$, $\mathbf{T^\alpha}$, $\mathbf{C^\alpha}$ and $\mathbf{A^L}$.

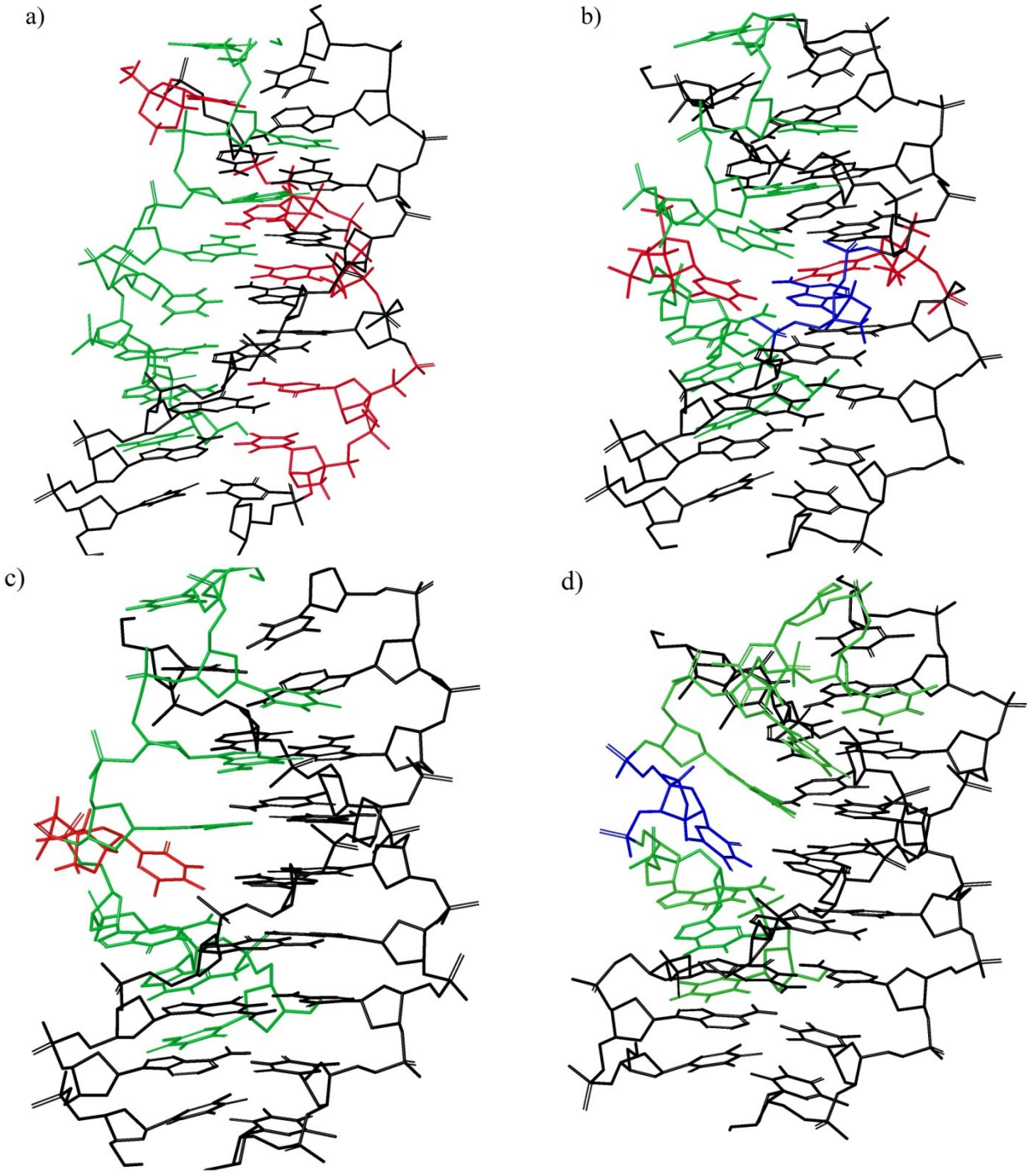

Fig. 10: Representative low-energy conformations of anti-parallel triplex (TFO the green color and Watson-Crick duplex the black color) containing insertion of LNA (blue color) and *α*-L-LNA (red color) produced by AMBER* calculations (**a**) *α*-L-LNA-T and *α*-L-LNA-C insertions in the target sequence, (**b**) *α*-L-LNA-T, LNA-A and *α*-L-LNA-T insertions as a base triplet in the TFO and duplex parts of the triplex. (**c**) *α*-L-LNA-T insertion in the TFO. (**d**) LNA-T insertion in the TFO.